Journal of Quantitative Spectroscopy & Radiative Transfer 245 (2020) 106840

Contents lists available at ScienceDirect

Journal of Quantitative Spectroscopy & Radiative Transfer

journal homepage: www.elsevier.com/locate/jqsrt

Water vapor absorption between 5690 and 8340 cm^{-1}: Accurate empirical line centers and validation tests of calculated line intensities

S.N. Mikhailenko[a,b], S. Kassi[c], D. Mondelain[c], A. Campargue[c,*]

[a] Laboratory of Theoretical Spectroscopy, V.E. Zuev Institute of Atmospheric Optics, SB, Russian Academy of Science, 1, Academician Zuev square, 634055 Tomsk, Russia
[b] Climate and Environmental Physics Laboratory, Ural Federal University, 19, Mira av., 620002 Yekaterinburg, Russia
[c] CNRS, LIPhy, Université Grenoble Alpes, 38000 Grenoble, France

ARTICLE INFO

Article history:
Received 5 November 2019
Revised 8 January 2020
Accepted 8 January 2020
Available online 11 January 2020

Keywords:
Water vapor
H_2O
Absorption spectroscopy
Cavity ring down spectroscopy
HITRAN
GEISA
Spectroscopic database

ABSTRACT

An accurate empirical list of 57,995 transitions is constructed for natural water in the 5690–8340 cm^{-1} near infrared region (1.76–1.20 μm). The new list represents an updated version of the list reported in Mikhailenko et al. (2016). The spectral range is extended to lower energy and the transition frequencies benefited from a series of recent measurements by comb-assisted cavity ring down spectroscopy (CA-CRDS).

The line list construction uses as starting point the variational line lists computed on the basis of the results of Schwenke and Partridge for the six most abundant water isotopologues ($H_2{}^{16}O$, $H_2{}^{18}O$, $H_2{}^{17}O$, $HD^{16}O$, $HD^{18}O$, $HD^{17}O$). Variational line positions are replaced by position values calculated from empirical rotation-vibration energy levels. The set of required empirical energy levels is improved in accuracy and enlarged, in particular for the minor isotopologues. A large number of energy levels and thus transition frequencies, relying on spectra recorded by CA-CRDS, have accuracy on the order of 10^{-4} cm^{-1}. All the transitions are provided with unique vibrational labeling supported by effective Hamiltonian calculations in case of ambiguity.

A detailed comparison is presented with the list of natural water included in the HITRAN2016 database and with the very recent $H_2{}^{16}O$ and $H_2{}^{18}O$ lists reported in Conway et al. (2020). The advantage of our list in terms of line position accuracy is demonstrated and illustrated by direct comparison with CRDS recordings at disposal. Intensity comparison shows a general agreement but a number of weaknesses of the most recent intensity calculations are evidenced. All the considered theoretical line lists include a few bands (*e.g.* $4\nu_2$, $5\nu_2$, $\nu_1+2\nu_2$ and $\nu_1+3\nu_2$) with intensities deviating significantly from the observations.

1. Introduction

In the two last decades, considerable progress has been achieved in the calculations of rovibrational spectra of small polyatomic molecules by *ab initio* and variational methods. Due to its importance for atmospheric applications, many works were devoted to a better characterization of the water absorption spectrum (see for instance Refs. [1–5]). Completeness, reasonable line position accuracy and good line intensity accuracy are the strong advantages of the variational line lists. Experimentally, the accurate measurement of hundreds thousands line intensities is out of reach in particular, for the water minor isotopologues while theoretical intensity values have, in general, similar accuracy for the main and minor isotopologues. As concerned line positions, theory cannot compete with experiment (except for H_2 and its isotopologues [6]). As a result, the general strategy for the best line list is to use as basis variational line lists and adjust line positions according to experimental values or to position values calculated from empirically determined energy levels. This method is that adopted for a large fraction of the water and carbon dioxide lists in the last edition of the HITRAN [7] and GEISA [8] databases.

Some years ago, under the project "A database of water transitions from experiment and theory", an IUPAC task group (IUPAC-TG) reported an exhaustive review and evaluation of rovibrational line positions, energy levels and assignments for the major isotopologues of water. By using the procedure and code MARVEL (Measured Active Rotational-Vibrational Energy Levels) [9,10], all the high quality absorption or emission line positions available in the literature at that time were used to determine and val-

* Corresponding author.
E-mail address: Alain.Campargue@univ-grenoble-alpes.fr (A. Campargue).

https://doi.org/10.1016/j.jqsrt.2020.106840
0022-4073/

idate empirical energy levels [11–13]. These cooperative efforts led to recommended set of energy level values with their self-consistent uncertainties. Since then, some deficiencies were evidenced in the quality of the determined levels and error bars. In particular, the inclusion in the MARVEL procedure of a considerable number of transition frequencies reported with underestimated error bars from poorly resolved emission spectra degraded the quality of part of the IUPAC-TG empirical levels. In addition, a few erroneous assignments in the original sources used by the IUPAC-TG could not be detected by the MARVEL procedure and affected the obtained values of the recommended levels.

Water vapor spectrum was the first high sensitivity spectrum that we recorded in 2004 with a newly built high sensitivity cavity ring down spectrometer. The use of a series of Distributed Feedback (DFB) laser diodes, each of them with 30 cm^{-1} tuning range, allowed for a full coverage of the 1.6 μm transparency window (6132–6748 cm^{-1}) [14]. Since then, the spectral coverage was extended over the wide 5690–8340 cm^{-1} range by using a collection of about one hundred DFB diodes [14–19] combined with an External Cavity Laser Diode (ECDL) in the 7920–8340 cm^{-1} region [20]. CRDS spectra of water vapor in natural isotopic abundance or enriched in D [21], ^{18}O [22] or ^{17}O [23–26] were recorded with increasing sensitivity and accuracy, over the last fifteen years. These spectra revealed a considerable number of new water lines. Those available at the date of the IUPAC-TG project were considered among the extensive sources of line positions used by the IUPAC-TG.

On the basis of these measurements [14–18,20–22] and absorption data available in the literature mostly for the strongest lines [27–37], in 2016, we released an empirical line list for the 5850–8340 cm^{-1} range [38]. This list corrected a number of deficiencies of the HITRAN2012 line list [39], in particular, the absence of many HDO lines of importance in the 1.6 μm window. Compared to the IUPAC-TG energy levels [11–13], new CRDS observations allowed extending the set of energy levels and correcting a number of inaccuracies. As a result, the GEISA database [8] reproduces our 2016 list in the considered region. The HITRAN2016 database [7] uses this list as main source of line positions of the main water isotopologue and reproduces part of the CRDS intensities. Let us underline the importance of the CRDS spectra at disposal for direct validation tests of the released water vapor lists. The available low pressure spectra of pure water vapor provide stringent tests to check the consistency of the empirical energy levels. This concerns in particular the large number of weak lines unobserved in atmospheric spectra or by Fourier Transform spectroscopy (FTS) associated with long path absorption (the weakest lines measured by CRDS have an intensity below 1×10^{-29} cm/molecule [18,20]).

In the present updated list, new experimental results obtained during the last four years are considered to further improve the accuracy of the line positions, extend the 2016 list down to 5690 cm^{-1} [19,23] and lower the intensity cut-off from 1×10^{-29} to 5×10^{-30} cm/molecule at 296 K. In particular, significant new information was retrieved from recordings performed with a sample with a highly enriched (~55 %) in ^{17}O:

(i) more than 1000 energy levels of $H_2{}^{17}O$ and $HD^{17}O$ were determined in the 1.6 μm transparency window (5850–6671 cm^{-1}) [24],
(ii) between 6667 and 7921 cm^{-1}, the spectra were recorded with a CRD spectrometer newly coupled to a self-referenced frequency comb (SRFC) providing accurate frequency value for each ring down event. The comb assisted CRDS method (CA-CRDS) allowed improving the accuracy of the line centers determination for the transitions of all water isotopologues contributing to the spectrum [25,26]. For instance, more than 5000 line positions of the main isotopologue were used to decrease the uncertainties of the previously known $H_2{}^{16}O$ energy levels. Test comparisons of energy level values determined from different transitions sharing the same upper level agree within a few MHz (~10^{-4} cm^{-1}) [26], more than one order of magnitude better than the average accuracy claimed for the positions retrieved from standard CRDS recordings (~10^{-3} cm^{-1}). In addition, hundreds of new energy levels of $H_2{}^{17}O$ and $HD^{17}O$ were determined from these recordings [25,26].
(iii) Finally, the new set of energy levels benefited from additional recent sources [40–43] including very accurate Lamb dip measurements [40] and some recent analysis of FTS spectra of ^{18}O [41] and ^{17}O [42] enriched water.

The rest of the paper is organized as follows. The line list construction is detailed in the next section. In Sections 3 and 4, we present a systematic comparison of the positions and intensities to the corresponding values included in the HITRAN2016 database for natural water and to very recent lists published by Conway et al. for $H_2{}^{16}O$ and $H_2{}^{18}O$ [44]. Several direct comparisons with the CRDS spectra at disposal will illustrate the advantages of our list. As concerned line intensities, a number of significant deviations between measurements, HITRAN2016 and variational intensities are discussed in Section 4.

2. Line list construction

All transitions stronger than 5×10^{-30} cm/molecule at 296 K of the variational line lists computed by Tashkun (IAO SB RAS, Tomsk, Russia) [45] on the basis of the results of Schwenke and Partridge (SP) [1,2] were gathered in a list for water in natural isotopic abundance. These 20 years old variational line lists are probably not the best-to-date variational lists (in particular for line positions) but they still have the unique advantage to be consistent for the six required isotopologues, to include reasonable rovibrational assignments and to be publicly available at http://spectra.iao.ru/.

The resulting SP list for natural water at 296 K between 5690 and 8340 cm^{-1} includes about 58,000 transitions with intensity larger than 5×10^{-30} cm/molecule for the six most abundant isotopologues ($H_2{}^{16}O$, $H_2{}^{18}O$, $H_2{}^{17}O$, $HD^{16}O$, $HD^{18}O$, and $HD^{17}O$). Contrary to the available calculated line lists and to the HITRAN list, all the transitions are provided with unique rovibrational assignment. Note that SP assignments were modified in some cases of strongly interacting rovibrational levels. These corrections were made according to calculations based on the effective Hamiltonian method. Details about these re-labelings can be found, for example, in Refs. [20,27,43]. Overall, the transitions belong to a total of 166 bands. We provide as Supplementary Material the band list with, for each band, the corresponding number of transitions, the spectral range and maximum values of J and K_a. A sample of the $H_2{}^{16}O$ band list is presented in Table 1 for 25 bands whose line intensities will be discussed in Section 4. An overview of the resulting list is compared to the HITRAN list in Fig. 1. Note that our intensity cut-off is twice lower than the HITRAN intensity cut-off (1×10^{-29} cm/molecule) but HITRAN2016 list includes $D_2{}^{16}O$ lines with intensities down to 1×10^{-32} cm/molecule.

As mentioned above, the variational line positions are replaced by values calculated from empirical rotation-vibration energy levels. The experimental sources used to construct our set of upper empirical energies are absorption spectra summarized in Table 2. High sensitivity CRDS measurements [14–26,36,37,40,43] were complemented by the results of Fourier transform [27–35,41,42] and ICLAS [46] measurements, in particular for the deuterated species. Note that more than half of the $H_2{}^{16}O$ transitions rely on the high precision line positions obtained by CA-CRDS [25,26,36,37,40]. The considered experimental sources

Table 1
Band-by-band statistics for twenty-five bands of the main water isotopologue contributing to the spectrum in the 5690–8340 cm^{-1} region. (The complete band list is provided as Supplementary Material.)

Rank	Band	Number of transitions	J_{max}	$K_{a\ max}$	Range/cm^{-1}
1	$2\nu_3$	2112	21	13	6207–8323
2	$2\nu_3-\nu_2$	334	15	8	5690–6236
3	$\nu_2+\nu_3$	708	21	13	5690–7183
4	$\nu_2+2\nu_3-\nu_2$	760	14	9	6465–8059
5	$2\nu_2+\nu_3$	2148	22	12	5761–8338
6	$2\nu_2+\nu_3-\nu_2$	190	16	10	5691–6297
7	$3\nu_2$	250	19	12	5691–7057
8	$3\nu_2+\nu_3$	512	18	8	7396–8339
9	$3\nu_2+\nu_3-\nu_2$	991	18	9	6077–7784
10	$4\nu_2$	1539	20	11	5695–8304
11	$4\nu_2+\nu_3-\nu_2$	245	14	6	7753–8340
12	$5\nu_2$	796	18	8	6375–8339
13	$\nu_1+\nu_3$	2631	23	14	6032–8327
14	$\nu_1+\nu_3-\nu_2$	243	15	9	5690–6178
15	$\nu_1+\nu_2$	491	19	13	5692–7210
16	$\nu_1+\nu_2+\nu_3$	204	20	8	7734–8340
17	$\nu_1+\nu_2+\nu_3-\nu_2$	1117	19	10	6355–7980
18	$\nu_1+2\nu_2$	1997	19	13	5912–8306
19	$\nu_1+3\nu_2$	552	18	9	6921–8339
20	$\nu_1+3\nu_2-\nu_2$	752	15	9	6102–7778
21	$\nu_1+4\nu_2-\nu_2$	288	13	6	7787–8338
22	$2\nu_1$	2324	21	13	6129–8319
23	$2\nu_1-\nu_2$	191	16	9	5690–6139
24	$2\nu_1+\nu_2$	164	17	10	7871–8339
25	$2\nu_1+\nu_2-\nu_2$	958	17	10	6375–7971

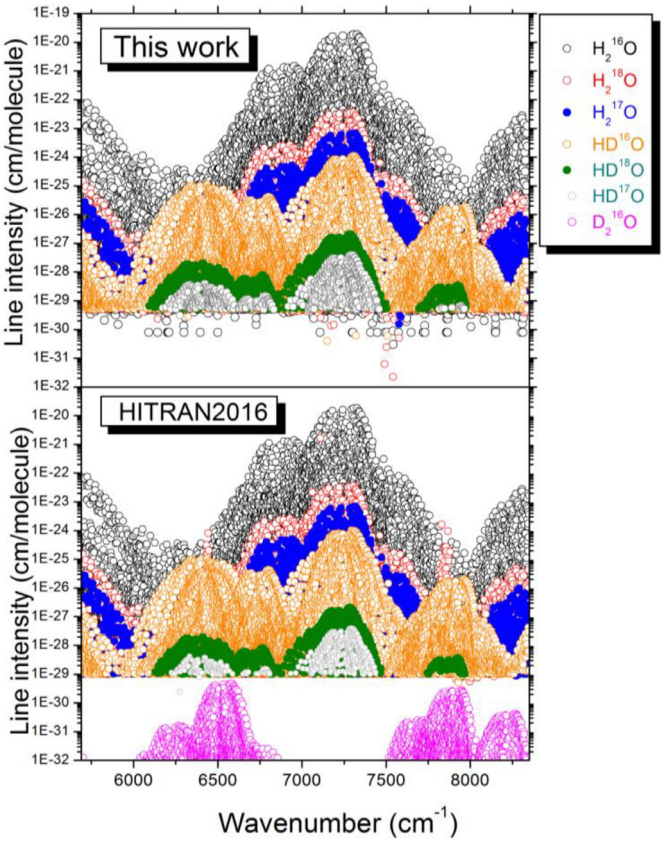

Fig. 1. Overview comparison between the list constructed in this work on the basis of the results of Schwenke and Partridge (SP) [1,2] and the HITRAN2016 line list for water vapor between 5690 and 8340 cm^{-1}.

[14–37,40–43,46] did not provide upper energy empirical values for about 6000 weak transitions (~10% in number representing only 1.6×10^{-4} of the total absorption). When available, we adopted the empirical energy levels recommended by the IUPAC-TG [11–13]. The energy levels adopted from the IUPAC-TG concern mostly very weak hot band transitions with an upper energy level determined from experimental studies at higher energy, not included among our sources of line positions (the most excited upper level involved in the list is the (121) $15_{2\ 14}$ level with an energy of about 12,902 cm^{-1}).

About 1750 transitions are left without empirical determination of their upper energy levels. For about 530 transitions reaching an upper level not yet observed, the frequencies could be estimated by *J, K* inter- or extrapolation of the deviations between empirical and SP variational positions of observed transitions of the considered bands. This procedure which was not implemented in the 2016 list [38] is believed to improve significantly SP variational positions. About 1200 (very weak) transitions (0.2%) were left with their SP variational positions.

As concerned the lower energy levels, the IUPAC-TG values were adopted for $H_2{}^{16}O$ [13] and $HD^{16}O$ [12]. For $H_2{}^{17}O$ and $H_2{}^{18}O$ isotopologues, we use rotational energies of the (000) and (010) states derived from hot emission FTS spectra of water vapor enriched in ^{17}O and ^{18}O [47]. The lower energies for the $HD^{18}O$ and $HD^{17}O$ species were calculated in Refs. [48,49] using an effective Hamiltonian approach [50].

At the final step of the line list construction, it appears that 282 very weak transitions of $H_2{}^{16}O$, $H_2{}^{18}O$, $HD^{16}O$ and $HD^{17}O$ with SP intensities below our 5×10^{-30} cm/molecule intensity cut-off are present in HITRAN2016 [7] or in the list of Conway et al. [44] with an intensity larger than 5×10^{-30} cm/molecule. For completeness, these transitions which may have underestimated SP intensities were added to the list with our empirical line positions.

In terms of accuracy only average estimates can be provided for the considered large amount of line positions. Experimentally, the line center accuracy depends on the accuracy of the calibration of the frequency axis and on the precision of the line center determination. The latter depends on the signal-to–noise ratio of the spectra, the blending with nearby lines, etc. Note that we consider here absorption spectra of pure water vapor at room temperature, thus with a pressure value on the order of 20 Torr at most. Nei-

Table 2
Number of transition frequencies between 5690 and 8340 cm^{-1} calculated from different upper energy sources.

	CA-CRDS [25,26,36,37]	Lamb dip [40]	CRDS [14–24,43]	FTS & ICLAS [27–35,41,42,46]	IUPAC [11–13]	Estimated	Variational [45]	**Total**
$H_2{}^{16}O$	12,646	84	2441	6528	3403	225	288	**25,615**
$H_2{}^{18}O$	4666		344	3013	553	114	287	**8977**
$H_2{}^{17}O$	5608		673	63	5	37	2	**6388**
$HD^{16}O$	1967		2610	8601	245	156	669	**14,248**
$HD^{18}O$	132			1708				**1840**
$HD^{17}O$	545		60	316		6		**927**
Total	**25,564**	**84**	**6128**	**20,229**	**4206**	**538**	**1246**	**57,995**

Note: According to the source of the upper level, the estimated accuracy of the transitions frequencies is the following: 2×10^{-4} cm^{-1} (CA-CRDS), 10^{-6} cm^{-1} (Lamb dip), 10^{-3} cm^{-1} (CRDS and FTS), 10^{-2} cm^{-1} (ICLAS and estimated) and a few tenth of wavenumber for SP.

Int_obs	Pos(SP)	Pos_empir	Int(SP)	E_low	ISO	Assignment	Source	Conway's Pos & Int	Conway's assignment	HITRAN2016 Pos & Int	HITRAN2016 assignment
	7448.5220	7448.522000	9.029E−30	2716.3293	HDO	002 19 2 17 000 18 3 16	variational				
	7448.5400	7448.540000	9.209E−30	2716.3293	HDO	002 19 3 17 000 18 3 16	variational			7448.5735 1.045E−29	
	7448.6642	7448.631000	2.829E−29	3629.0943	H2O	101 15 9 7 000 15 7 8	estimated	7449.2351 2.754E−29		7449.2351 2.806E−29	101 15 9 7 000 15 7 8
	7448.7192	7448.637400	4.283E−28	1875.4693	H2O	031 5 5 0 010 4 1 3	FTS	7448.6350 4.522E−28		7448.6374 4.300E−28	
	7448.7220	7448.722000	5.666E−30	2873.3223	H2018	200 15 5 11 000 14 4 10	variational	7448.8730 5.372E−30	−222 15 −2 −2 000 14 4 10		
	7448.8214	7448.769600	9.423E−28	1774.6153	H2O	002 11 4 8 000 12 1 11	CRDS	7448.7701 9.475E−28		7448.7699 9.200E−28	
	7448.7278	7448.804720	7.779E−31	1360.2350	H2O	120 9 7 2 000 9 4 5	CA-CRDS	7448.8041 1.082E−29			
	7448.8790	7448.840200	1.977E−29	3935.3448	H2O	003 4 3 1 100 3 3 0	FTS	7448.8390 1.977E−29		7448.8402 1.971E−29	
	7449.1128	7448.885120	2.000E−29	1119.4883	H2017	101 8 6 2 000 8 4 5	CA-CRDS			7448.8852 2.000E−29	
	7449.1776	7448.929140	1.256E−27	1055.2554	H2017	002 8 4 5 000 7 5 2	CA-CRDS			7448.9299 1.740E−27	
	7448.9727	7448.934910	4.678E−28	604.5442	H2018	002 6 3 3 000 5 4 2	CA-CRDS	7448.9359 5.124E−28		7448.9359 5.510E−28	
2.828E−26	7448.9625	7448.981600	3.272E−26	2927.9399	H2O	101 14 7 7 000 13 7 6	CA-CRDS	7448.9815 3.219E−26		7448.9821 2.830E−26	
	7448.9738	7449.020400	5.042E−28	2416.7832	H2018	101 14 4 11 000 13 4 10	CRDS	7449.0200 5.000E−28		7449.0194 4.430E−28	
	7449.0428	7449.043000	1.038E−29	4184.8299	H2O	130 15 4 11 010 14 3 12	variational	7449.1490 1.036E−29	−222 15 −3 −3 010 14 3 12	7449.2451 1.010E−29	−222 15 −3 −3 010 14 3 12
	7449.1176	7449.087500	9.061E−28	752.1874	H2018	002 7 3 5 000 6 4 2	CA-CRDS	7449.0885 1.041E−27		7449.0885 1.160E−27	
	7449.2336	7449.108650	5.422E−28	325.8804	H2017	200 6 2 4 000 5 1 5	CA-CRDS			7449.1088 5.950E−28	
	7449.3113	7449.142920	2.497E−27	753.7052	H2017	200 7 5 2 000 6 4 3	CA-CRDS			7449.1419 2.180E−27	
	7449.2013	7449.239860	7.118E−27	2813.5273	H2O	101 13 8 5 000 12 8 4	CA-CRDS	7449.2424 6.983E−27		7449.2407 6.984E−27	
	7449.2513	7449.251980	4.119E−26	885.6002	H2O	101 8 4 4 000 8 2 7	CA-CRDS	7449.2518 4.538E−26		7449.2518 4.279E−26	
	7449.2230	7449.255060	1.535E−25	1813.2226	H2O	021 12 5 7 000 11 3 8	CA-CRDS	7449.2535 1.578E−25		7449.2541 1.558E−25	
	7449.3471	7449.280500	5.204E−30	2388.0297	HDO	012 10 5 6 010 9 4 5	FTS				
	7449.3630	7449.318500	3.841E−28	1080.3853	H2O	050 8 1 7 000 9 2 8	CA-CRDS	7449.3194 5.321E−28		7449.3198 4.410E−28	
	7449.3189	7449.319000	8.942E−30	2715.5327	HDO	002 19 2 17 000 18 2 16	variational			7449.3582 1.016E−29	
	7449.3370	7449.337000	9.004E−30	2715.5327	HDO	002 19 3 17 000 18 2 16	variational				
	7449.4237	7449.356500	2.991E−29	3796.5397	H2O	003 4 1 4 100 3 1 3	FTS	7449.3549 2.988E−29		7449.3564 2.982E−29	
	7449.4225	7449.485700	7.247E−28	2595.8127	H2O	012 8 3 5 010 8 2 6	FTS	7449.4849 6.670E−28		7449.4849 6.510E−28	
3.390E−26	7449.4469	7449.487520	3.681E−26	1813.2226	H2O	200 11 6 5 000 11 3 8	CA-CRDS	7449.4871 3.520E−26		7449.4879 3.671E−26	
	7449.3754	7449.489200	1.042E−29	4728.2197	H2O	111 16 3 13 010 15 3 12	IUPAC	7449.4892 1.036E−29		7449.4892 1.037E−29	
	7449.8300	7449.497420	1.116E−29	1996.8541	H2017	031 6 5 1 010 5 1 4	CA-CRDS			7449.4995 1.120E−29	
	7449.3149	7449.656000	7.854E−29	2471.2550	H2O	120 10 10 0 000 10 9 1	IUPAC	7449.6565 8.011E−29	040 10 10 0 000 10 9 1	7449.3315 7.722E−29	040 10 10 0 000 10 9 1
	7449.3138	7449.656400	2.370E−28	2471.2546	H2O	120 10 10 1 000 10 9 2	IUPAC	7449.6569 2.403E−28	040 10 10 1 000 10 9 2	7449.3315 2.317E−28	040 10 10 1 000 10 9 2
	7449.6956	7449.682190	3.810E−26	94.7886	H2018	002 2 2 0 000 2 1 1	CA-CRDS	7449.6823 3.670E−26		7449.6826 3.630E−26	
	7449.7582	7449.774430	1.678E−24	1985.7842	H2O	101 12 5 8 000 11 5 7	CA-CRDS	7449.7747 1.658E−24		7449.7748 1.640E−24	
	7449.8542	7449.822760	6.662E−30	1437.9678	H2O	021 10 6 5 000 10 5 8	CA-CRDS	7449.8232 1.050E−29			
	7449.8259	7449.881700	1.658E−28	2939.9563	H2018	101 17 2 16 000 16 2 15	CRDS	7449.8800 1.644E−28		7449.8808 2.200E−28	
	7449.8341	7449.888000	5.526E−29	2939.9470	H2018	101 17 1 16 000 16 1 15	estimated	7449.9889 5.482E−29	−222 17 −2 −2−222 16 −2 −2		
	7449.8004	7449.895100	3.978E−29	1814.0870	H2018	012 4 2 3 010 4 1 4	FTS	7449.8955 3.644E−29		7449.8951 3.980E−29	
1.859E−26	7449.9009	7449.933460	2.048E−26	2813.5114	H2O	101 13 8 6 000 12 8 5	CA-CRDS	7449.9336 2.010E−26		7449.9336 2.011E−26	

Fig. 2. Sample of the line list provided as Supplementary Material. The different columns are: Int_obs – line intensity at 296 K (cm/molecule) measured from the CRDS spectrum of natural water [16–20] (the listed values are limited to well isolated $H_2{}^{16}O$ lines with intensity larger than 10^{-27} cm/molecule); Pos(SP) – variational line center from Schwenke and Partridge results (cm^{-1}); Pos_empir – empirical value of the line center (cm^{-1}); Int(S) – SP variational line intensity [1,2,45]; E_low – lower state energy level (cm^{-1}); ISO – isotopologue; Assignment – upper and lower level rovibrational assignments; Source – source of our empirical value of the upper energy level; Conway Pos & Int – line center and line intensity at 296 K reported by Conway et al. [44] (for $H_2{}^{16}O$ and $H_2{}^{18}O$ transitions); Conway's assignment – rovibrational assignment given only when it differs from ours; "HITRAN2016 Pos & Int" and "HITRAN2016 assignment" – same for the HITRAN database [7].

ther in the present study nor in the MARVEL treatment followed by the IUPAC-TG, the position values were corrected from the self-pressure shifts. Self-pressure shift coefficients vary typically in the $\pm 10^{-2}$ cm^{-1} atm^{-1} range which leads to typical shifts on the order of 10^{-4} cm^{-1} ($\sim$ 3 MHz) which is small in general but may be significant compared to the accuracy of the CA-CRDS line centers. Additional biases related to the choice of the line shape used to fit the measured line profile are also expected to affect the line center determination but these effects are smaller. Most of the line centers were obtained using the standard Voigt profile. Significant residuals are generally obtained showing the typical W signature due to the Dicke narrowing effect [51]. Nevertheless, the obtained residuals are generally symmetric indicating that the line center determination is mostly unaffected.

We present in Table 3 some examples of determinations of the upper energy levels from line centers of different transitions measured by CA-CRDS. An extended version of Table 3 is given as Supplementary Material. Similar accuracy tests included in Ref. [26] relative to the 6900–7400 cm^{-1} region, showed a consistency at the 10^{-4} cm^{-1} level between the various determinations. Here, together with line positions of Ref. [26], we consider the transition frequencies reported in the 7400–7920 cm^{-1} region [25] which enlarges importantly the possibilities of redundant determinations of a given upper level. A similar agreement on the order of 10^{-4} cm^{-1} is achieved, illustrating the consistency of the frequencies measured in Refs. [25,26]. As a result, the average accuracy for transition frequencies derived from well isolated lines measured by CA-CRDS [25,26] is estimated to be 2×10^{-4} cm^{-1}. For standard CRDS and FTS, an uncertainty of 10^{-3} cm^{-1} as given in Ref. [38] is a reasonable average value. For ICLAS line positions [46] and those estimated using an *J,K* empirical law correction of their SP positions, the uncertainty is on the order of 10^{-2} cm^{-1}. Finally, for the very small fraction of purely SP variational positions [45] included in our list, various comparisons with experimental values have shown that in our region, SP positions may deviate by a few tenth of wavenumber (see below). The most accurate line positions are those related to the ten Lamb dip measurements reported in Ref. [40] which allowed computing 84 line positions with an accuracy of about 10^{-6} cm^{-1} (30 kHz). In the line list provided as Supplementary Material, the source of the upper energy level is provided for each transition. The number of decimal digits provided for each position has been adapted according to the estimated uncertainties (for instance, five and six digits for the values relying on CA-CRDS and Lamb dips, respectively).

Fig. 2 shows a sample of the line list provided as Supplementary Material. Together with the recommended position and corresponding source, the list includes our rovibrational assignment, SP intensity, the lower state energy value and the corresponding HITRAN [7] and Conway et al. [44] values for the positions and intensities. When a different rovibrational assignment was proposed by Conway et al. or in HITRAN2016 list, it is included for comparison. This global line list gathering most of the information at disposal was used for the systematic comparisons presented below.

In our region, the HITRAN list includes 48,692 transitions for the six major water isotopologues. Although the HITRAN intensity cut-off is 1×10^{-29} cm/molecule, 40 transitions have an intensity below this value, down to 1.1×10^{-37} cm/molecule for the $5\nu_2$ $4_{4\,0} - 4_{1\,3}$ transition of $HD^{17}O$. In addition, many transitions of the $D_2{}^{16}O$ isotopologue with intensity below 1×10^{-29} cm/molecule are included in the HITRAN list (see Fig. 1).

For the main isotopologue (about 21,500 transitions), HITRAN position and intensity values were taken from six and nine sources, respectively. More than 80% of the positions are empirical values transferred from our 2016 list [38]. The remaining $H_2{}^{16}O$ positions are empirical from the IUPAC-TG (9.7%) [13] or measured by FTS values from Toth's database (6.4%) [54], with a very small fraction of variational values and a few values with uncertain origin. As concerned $H_2{}^{16}O$ line intensities, about 74% of them have variational origin [52,53] and 17% are CRDS intensity values from Refs. [16,17,20].

The $H_2{}^{16}O$ and $H_2{}^{18}O$ lists published by Conway et al. [44] have intensities calculated using an *ab initio* dipole moment surface [4]. They were found to show a better agreement with experiment than the preceding 'POKAZATEL' line list [55]. In the 5690–8340 cm^{-1} interval, Conway list includes 32,553 $H_2{}^{16}O$ transitions above an intensity cut-off fixed to 1×10^{-30} cm/molecule at 296 K. Note that the maximum *J* value of the lower and upper levels is 20 while our list includes transitions with *J* values up to 22 and 23 for $H_2{}^{16}O$ and $H_2{}^{18}O$, respectively (the $\nu_1+\nu_3$ $21_{1\,21} - 20_{1\,20}$ line at 7485.3914 cm^{-1} has for instance an intensity of about 5×10^{-28} cm/molecule significantly above the intensity cut-off).

Table 3
Comparison of various determinations of upper energy levels obtained from the line centers of transitions measured by CA-CRDS in Refs. [25,26]. In the last column, the average value is given with the corresponding standard deviation in the unit of the last quoted digit.

ISO	Line position (cm^{-1})	$(V_1V_2V_3)$ J' Ka' Kc'	J'' Ka'' Kc''	Upper energy (cm^{-1})	Average value (cm^{-1})
$H_2{}^{16}O$	7843.31579	002 7 5 3	6 2 4	8446.08928	8446.08928(1)
	7688.30913		6 4 2	8446.08928	
	7401.03099		6 6 0	8446.08926	
	7518.34542		7 4 4	8446.08929	
	7421.24093	021 10 2 8	9 0 9	8341.40891	8341.40883(1)
	7047.77501		10 2 9	8341.40870	
	6760.07327		10 4 7	8341.40895	
	7014.29919		11 0 11	8341.40876	
	7356.64521	040 10 5 6	9 0 9	8276.81319	8276.81318(3)
	6983.17951		10 2 9	8276.81320	
	6695.47753		10 4 7	8276.81322	
	6949.70358		11 0 11	8276.81315	
	7708.32176	101 11 5 7	10 3 8	9154.44964	9154.44958(5)
	7435.73114		10 5 6	9154.44960	
	7629.60228		11 1 10	9154.44954	
	7155.45478		11 5 6	9154.44959	
	6832.54451		11 7 4	9154.44952	
$H_2{}^{18}O$	7508.72473	002 5 0 5	4 1 4	7732.55306	7732.55312(5)
	7226.82448		5 3 2	7732.55311	
	7287.20719		6 1 6	7732.55318	
	7087.17071		6 3 4	7732.55314	
	7462.95544	101 6 3 3	5 1 4	7861.31580	7861.31585(4)
	7215.93340		6 3 4	7861.31583	
	6981.23971		6 5 2	7861.31590	
	7021.76646		7 3 4	7861.31587	
	7190.39940	200 4 1 4	3 2 1	7401.19840	7401.19850(10)
	7102.57855		4 2 3	7401.19847	
	7077.15196		5 0 5	7401.19850	
	6956.04030		5 2 3	7401.19864	
$H_2{}^{17}O$	7905.61486	002 10 3 8	9 0 9	8823.71701	8823.71721(13)
	7623.75408		9 2 7	8823.71713	
	7466.16140		9 4 5	8823.71742	
	7532.91852		10 2 9	8823.71721	
	7246.02895		10 4 7	8823.71726	
	6955.38672		10 6 5	8823.71715	
	7136.33442		11 2 9	8823.71731	
	7360.16472	021 7 5 2	6 3 3	8020.15178	8020.15170(14)
	7136.03758		6 5 1	8020.15165	
	6965.09732		7 5 3	8020.15153	
	6971.49441		8 3 5	8020.15165	
	6768.86048		8 5 3	8020.15189	
	7569.80437	101 7 4 4	6 2 5	8121.41406	8121.41389(13)
	7536.47287		7 0 7	8121.41396	
	7340.03635		7 2 5	8121.41382	
	6911.59545		7 6 1	8121.41372	
	6716.26598		8 6 3	8121.41388	
	7378.14358	111 4 2 2	3 0 3	9106.40406	9106.40400(5)
	7291.32478		3 2 1	9106.40395	
	7202.83474		4 2 3	9106.40402	
	7056.69185		5 2 3	9106.40398	
	7568.63956	200 8 4 5	7 1 6	8271.52554	8271.52558(4)
	7430.66057		7 3 4	8271.52563	
	7267.74419		8 3 6	8271.52557	
	7021.02696		8 5 4	8271.52558	
$HD^{16}O$	7301.24803	002 3 1 3	2 0 2	7347.42114	7347.42117(15)
	7289.29444		2 1 2	7347.42132	
	7238.15185		2 2 0	7347.42094	
	7197.26499		4 0 4	7347.42130	
	7191.03890		4 1 4	7347.42116	
	7313.67622	002 4 1 3	3 1 2	7430.13757	7430.13743(12)
	7279.98112		4 0 4	7430.13743	
	7208.30111		4 2 2	7430.13728	
	7136.50091		5 2 4	7430.13744	
	7429.45104	002 7 4 4	6 3 3	7899.11465	7899.11462(6)
	7325.22399		6 4 3	7899.11467	
	7322.20986		7 3 5	7899.11454	
	7090.55168		8 4 5	7899.11460	
$HD^{17}O$	7277.85690	002 3 1 3	2 1 2	7335.70340	7335.70351(12)
	7186.05778		4 0 4	7335.70358	
	7179.94164		4 1 4	7335.70364	
	7114.85032		4 2 2	7335.70342	
	7377.68464	002 5 2 3	4 1 4	7533.44664	7533.44657(18)
	7312.59336		4 2 2	7533.44646	
	7160.94208		5 3 2	7533.44638	
	7131.34089		6 2 4	7533.44679	
	7430.42693	002 7 5 2	6 4 3	8001.19483	8001.19494(15)
	7296.30045		6 5 1	8001.19495	
	7321.02464		7 4 3	8001.19514	
	7187.79783		7 5 3	8001.19483	

In our region, the $H_2{}^{18}O$ list of Conway includes 9191 transitions with intensity (including the abundance factor) larger than 5×10^{-30} cm/molecule (to be compared to 8977 in our list). 263 of them are duplicate (same position, same intensity, same assignment) which should be removed. In the whole Conway $H_2{}^{18}O$ line list (100% abundance for the line intensities) extending up to 20,000 cm^{-1}, we could identify 5394 such duplicates.

The systematic comparison to HITRAN and Conway lists is not straightforward because these two references do not provide complete rovibrational assignments for part of the transitions. For instance, in our region, 1442 $H_2{}^{16}O$ transitions of the Conway list are provided with incomplete rovibrational assignment of the upper level. In those circumstances, the transitions in common with our list were identified by using as criteria identical lower state energy, identical upper *J* value and reasonable position and intensity matching (typically 0.5 cm^{-1} and a factor of 2, respectively). We have included in the Supplementary Material the position and intensity columns for the HITRAN and Conway transitions in coincidence (see Fig. 2). When a different or incomplete rovibrational assignment was attached to the considered transition, it is reproduced. HITRAN erroneous assignments include more than 160 ortho-para transitions between 6048 and 8233 cm^{-1} which are strictly forbidden by symmetry (all of them were erroneously referenced to our 2016 list [38] in the HITRAN database).

As mentioned above less than 300 very weak lines (intensity smaller than 1.6×10^{-27} cm/molecule) present in the list of Conway et al. or HITRAN with intensity larger than our 5×10^{-30} cm/molecule intensity cut-off but with SP intensities below 5×10^{-30} cm/molecule, were added to our list (these transitions with SP intensity smaller than 5×10^{-30} cm/molecule are visible on the upper panel of Fig. 1).

More significant is the fact that our list based on SP results includes a number of $H_2{}^{16}O$ transitions missing in the HITRAN list and to a lesser extend in the list by Conway et al., some of them with relatively high intensity (see Fig. 3). HITRAN list misses a few medium $H_2{}^{16}O$ transitions with intensity up to 1.6×10^{-25} cm/molecule (for the $2\nu_3$ $8_{7\,2}$ – $8_{6\,3}$ line at 7514.916 cm^{-1}) and a large set of weak transitions with intensity below 5×10^{-28} cm/molecule. As concerned the list by Conway et al., only about 50 weaker lines are missing, half of them corresponding to *J* values larger than 20. Both lists are practically complete for the $H_2{}^{18}O$ isotopologue. Fig. 4 shows two examples of CRDS spectra of natural water in spectral intervals where relatively strong $H_2{}^{16}O$ lines are missing in HITRAN.

3. Line position comparison

Fig. 5 presents an overview of the differences between our position values and those of our 2016 list [38], in HITRAN2016 [7], by Conway et al. [44], and the SP variational values [45]. The comparison is limited to the three first isotopologues and the position differences are plotted *versus* the line intensity in order to distinguish the weak lines for which experimental positions are less accurate. Note that the comparison applies only to the lines for which an empirical value of the upper energy level was determined by CA-CRDS, CRDS or FTS (the line positions of our list with IUPAC-TG, estimated or variational position values are thus excluded from the comparison). As expected SP variational positions show relatively large deviations. It is worth noting that SP average deviations are close to zero for $H_2{}^{16}O$ and $H_2{}^{18}O$ while $H_2{}^{17}O$ SP positions are systematically overestimated by about 0.25 cm^{-1}.

Compared to the 2016 list, a significant number of deviations are noted for the two minor isotopologues (in particular $H_2{}^{17}O$). This is due to the recent extension of the set of empirical energy levels of these two species [23–26,41–43]. Most of the large deviations are related to newly determined energy levels for which SP

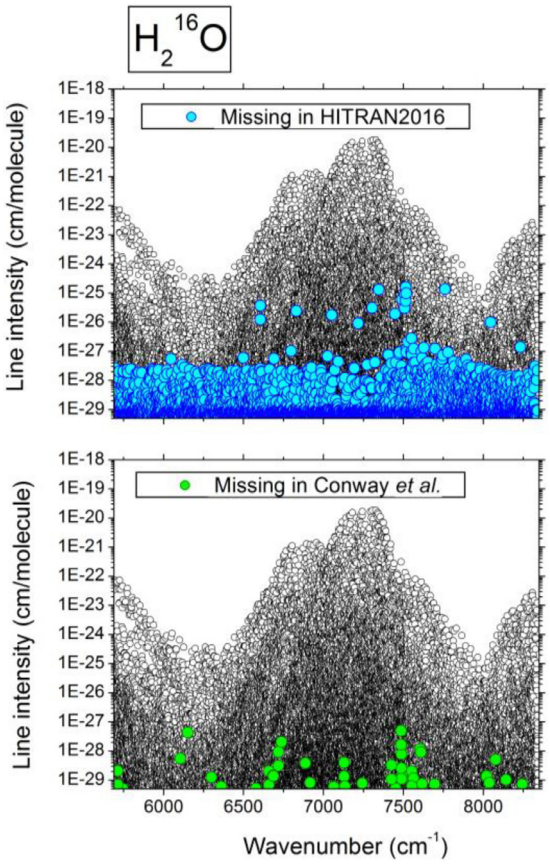

Fig. 3. Overview of the transitions missing in the $H_2{}^{16}O$ lists provided by the HITRAN2016 [7] database (upper panel) and Conway et al. [44] (lower panel). Missing transitions are highlighted in light blue and green, respectively.

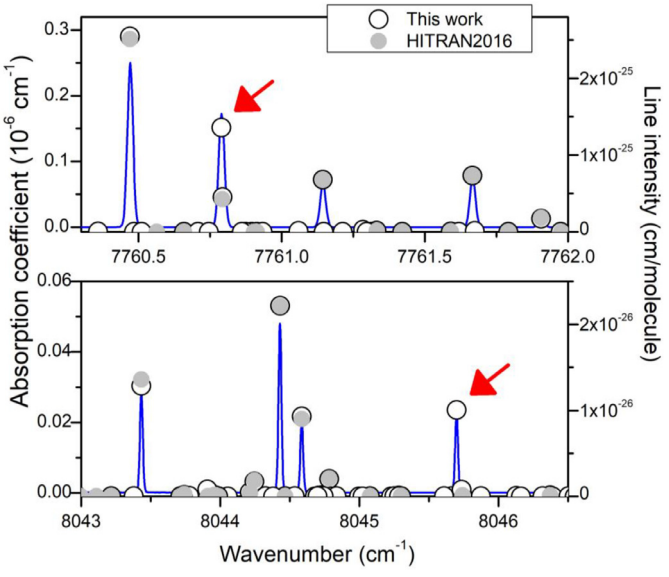

Fig. 4. Relatively strong $H_2{}^{16}O$ lines missing in the HITRAN2016 list (red arrows). The present line list (open circles) is superimposed to the CRDS spectrum of natural water [16,20] (blue solid line).

variational values were used in the 2016 list (see for instance the set of large positive deviations around 0.25 cm^{-1}, with SP origin, observed for $H_2{}^{17}O$).

Fig. 5 illustrates the good agreement of the present and HITRAN positions of the main isotopologue. This simply reflects the fact that our 2016 list was adopted as HITRAN source for about 80%

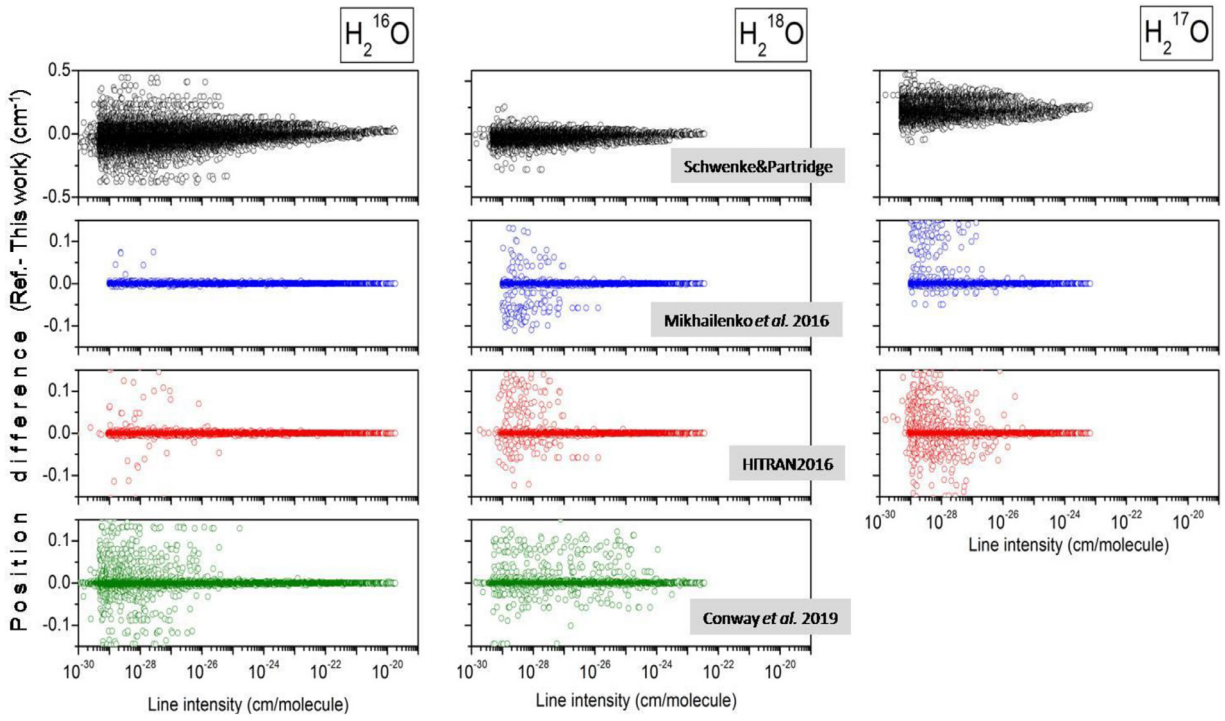

Fig. 5. Overview of the deviations between our position values and the values provided in different references.
From top to bottom: Schwenke and Partridge (black) [1,2,45], our 2016 list (blue) [38], HITRAN2016 (red) [7] and Conway et al. (green) [44]. Note the different scale used for SP deviations because SP positions are less accurate variational values while, for the other sources, most of the positions were empirically corrected.

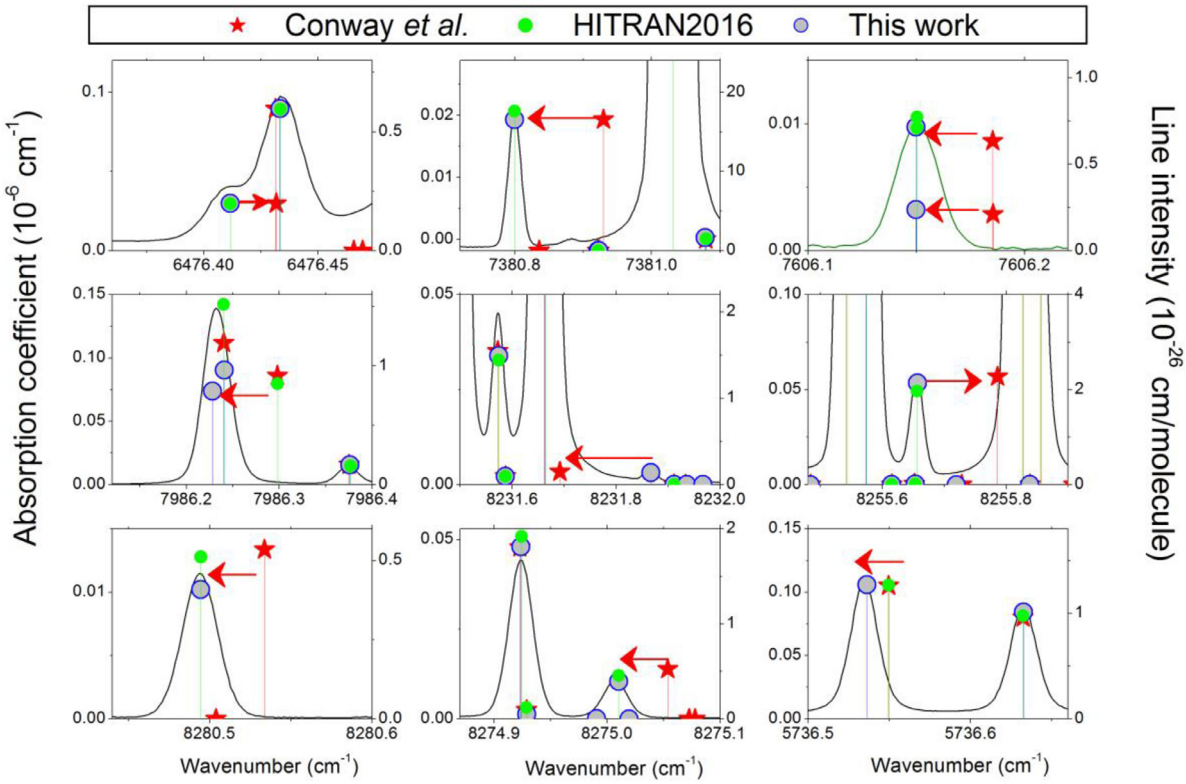

Fig. 6. Inaccurate positions of $H_2{}^{16}O$ lines in the list by Conway et al. [44] and in the HITRAN2016 list (red stars and full green circles, respectively). The present line list (full grey circles) is superimposed to the CRDS spectrum of natural water [16–20].

of the $H_2{}^{16}O$ positions in the region. For the $H_2{}^{18}O$ and $H_2{}^{17}O$ positions, a significant number of deviations are noted mostly due to variational position values used in HITRAN. Among the six sources used for HITRAN2016 positions in the region, most of the important deviations compared to the present position values are related to a variational value of the upper level, an erroneous determination of the IUPAC-TG energy level or some Toth's values [54]. For instance, the maximum deviation ($\delta\nu = 4.898$ cm^{-1}) concerns the $\nu_1+2\nu_2$ $12_{1\ 12}$ – $12_{2\ 11}$ transition observed at 6511.519 cm^{-1} [14,18] but reported by Toth [54] at 6516.418 cm^{-1}. Note that this last line corresponds in fact to the $\nu_1+3\nu_2-\nu_2$ $7_{1\ 7}$ – $8_{0\ 8}$ hot transition. Transition frequencies reaching the (040) $14_{8\ 6}$ upper level shows inconsistencies: while the HITRAN line positions of the $4\nu_2$ $14_{8\ 6}$ – $13_{5\ 9}$ (7781.700 cm^{-1}), $14_{8\ 6}$ – $13_{7\ 7}$ (7441.155 cm^{-1}) and $4\nu_2-\nu_2$ $14_{8\ 6}$ – $13_{1\ 13}$ (6977.101 cm^{-1}) transitions coincide with our values, the $4\nu_2$ $14_{8\ 6}$ – $15_{1\ 15}$ (8010.110 cm^{-1}) transitions deviates by 0.182 cm^{-1}. The line positions of the first three line centers were taken from our 2016 database [38] while the inaccurate position value is a variational value [48] provided without complete vibration-rotation assignment in HITRAN.

Unexpectedly, the $H_2{}^{16}O$ and $H_2{}^{18}O$ positions very recently reported by Conway et al. [44] show larger deviations than the HITRAN2016 positions. No information is given by Conway et al. about the experimental sources used to determine their MARVEL energy levels. This lack of knowledge (and recognition) of the experimental results considered in the "MARVELization" of the measured transition frequencies hinders to trace the origin of these inaccurate line positions. The present analysis does not support the proposition of Conway et al. to use their $H_2{}^{16}O$ and $H_2{}^{18}O$ lists to update the water vapor line list in the next edition of the HITRAN database [44].

Nine examples of $H_2{}^{16}O$ transitions with inaccurate positions in the list of Conway et al. are illustrated on Fig. 6 and compared to CRDS spectra of natural water [16–20]. The chosen examples sample the entire 5690–8340 cm^{-1} range. The HITRAN stick spectrum superimposed on the plots (green circles) indicates that for only two of the nine plotted examples, HITRAN2016 positions disagree with the CRDS spectra. The two inaccurate HITRAN frequencies are those of the $\nu_1+\nu_2$ $15_{6\ 10}$ – $14_{5\ 9}$ and $5\nu_2$ $11_{3\ 9}$ – $12_{0\ 12}$ transitions at 5736.5361 and 7986.2015 cm^{-1}, respectively. Their positions were computed using inaccurate empirical IUPAC-TG energy of the (110) $15_{6\ 10}$ and (050) $11_{3\ 9}$ upper levels, respectively [13]. Correct values of the considered frequencies were included in our 2016 list [38].

4. Line intensity comparison

Our 2016 list [38] includes experimental values of line intensities when available. FTS [27,54] and CRDS [14–18,20,37] intensity values were used for the strong lines and weaker lines, respectively (see Fig. 5 of Ref. [38]). Similarly to the present work, the list was made complete by including a number of weak transitions not yet measured, with empirical positions and SP variational intensities. Note that part of the same sets of FTS and CRDS intensity values are incorporated in the HITRAN2016 list. A discussion about the relative merit of experimental and variational line intensities was included in Ref. [38] and is not repeated here.

Overall a set of more than 20000 line intensities were measured by CRDS in Refs. [14–18,20] but no individual error bars were attached to this large set of measurements. In the case of well-isolated $H_2{}^{16}O$ lines of intermediate intensity, a 2–5% relative accuracy was uniformly estimated [38] but the lines in questions were not listed. In the present work, we examined in details the spectra and selected the isolated $H_2{}^{16}O$ lines for which the intensity determination is believed to be the most reliable. Only lines with intensity larger than 1×10^{-27} cm/molecule were considered. The following comparison is thus limited to these selected intensity values, about 5000 in total, which are included in the Supplementary Material (see Fig. 2). Note that in the 7408–7920 cm^{-1} strong absorption region [16], low pressure values (≈0.1 Torr) were used for the CRDS recordings and a systematic error due to the pressure gauge calibration was evidenced [16,37]. This systematic bias was corrected by applying a 1.044 multiplication factor to the intensities in the considered region (as done in the 2016 list [38]).

Fig. 7 presents an overview of the ratios of SP, HITRAN and Conway et al. intensities to the CRDS values of the 5000 selected

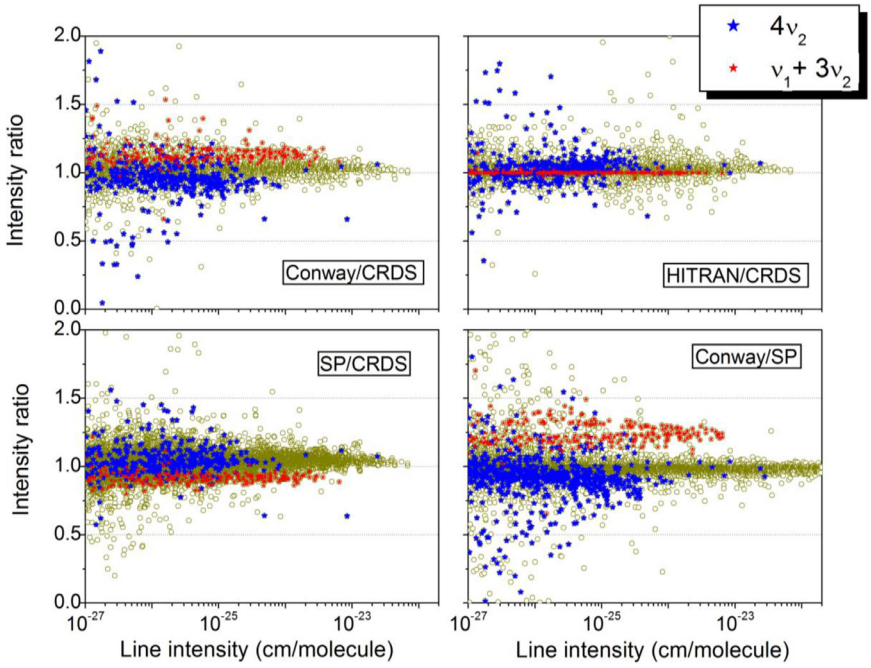

Fig. 7. Intensity ratios for the $H_2{}^{16}O$ main isotopologue (olive circles). The values relative to the $4\nu_2$ and $\nu_1+3\nu_2$ transitions are highlighted (blue and red stars, respectively). The CRDS values are limited to lines of Refs. [16–20] with intensity larger than 10^{-27} cm/molecule not affected by strong blendings with nearby lines (see text).

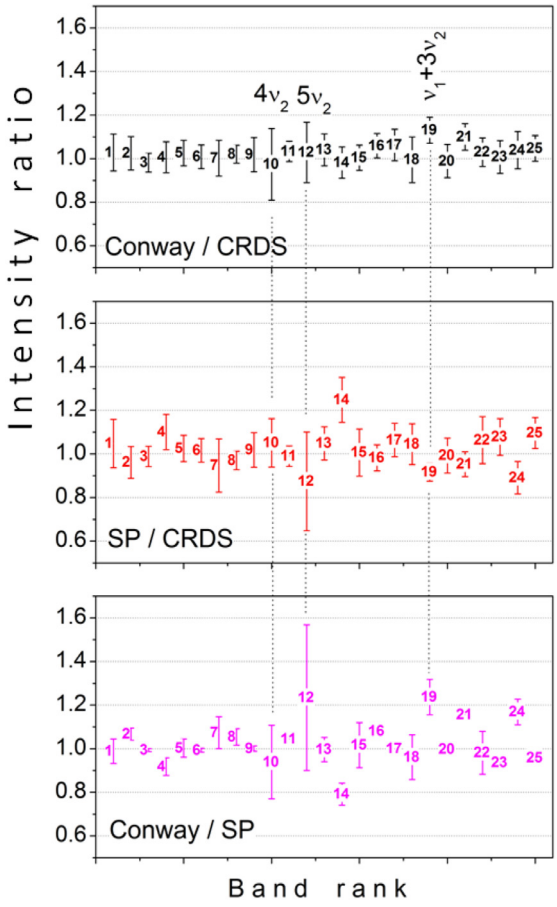

Rank	Band
1	$2\nu_3$
2	$2\nu_3$-ν_2
3	ν_2+ν_3
4	ν_2+$2\nu_3$-ν_2
5	$2\nu_2$+ν_3
6	$2\nu_2$+ν_3-ν_2
7	$3\nu_2$
8	$3\nu_2$+ν_3
9	$3\nu_2$+ν_3-ν_2
10	$4\nu_2$
11	$4\nu_2$+ν_3-ν_2
12	$5\nu_2$
13	ν_1+ν_3
14	ν_1+ν_3-ν_2
15	ν_1+ν_2
16	ν_1+ν_2+ν_3
17	ν_1+ν_2+ν_3-ν_2
18	ν_1+$2\nu_2$
19	ν_1+$3\nu_2$
20	ν_1+$3\nu_2$-ν_2
21	ν_1+$4\nu_2$-ν_2
22	$2\nu_1$
23	$2\nu_1$-ν_2
24	$2\nu_1$+ν_2
25	$2\nu_1$+ν_2-ν_2

Fig. 8. Average intensity ratios for twenty-five bands of the $H_2{}^{16}O$ main isotopologue (olive circles). Each band is tagged with a number indicated on the plots, the correspondence being given in the right-hand table. The plotted error bars correspond to the *rms* deviation of the ratios. (Numerical values are provided as Supplementary material.)

$H_2{}^{16}O$ lines. Most of the HITRAN intensities have variational origin (from the BT2 [52] and Lodi et al. [53] line lists) but part of the CRDS intensity values [16,17,20,36,37] were adopted in the HITRAN list. A larger uncertainty on the experimental intensities of the weak lines is not believed to be the only reason of the increasing dispersion of the ratios observed for the smaller intensities. Indeed, the comparison between SP intensities and the *ab initio* intensities by Conway et al. [44] shows similar or even larger scattering (Fig. 7). Let us mention that the observed intensity disagreements cannot be explained by differences in the assignments in the considered line lists because the vast majority of the assignments are confirmed by lower state combination relations. For only 49 lines among the set of 5000 lines, the vibrational labeling in Conway's list does not coincide with ours.

As the quality of the calculations is known to depend on vibrational bands, it is worth comparing separately the intensities of the different bands. We provide as Supplementary Material a series of comparison for 25 $H_2{}^{16}O$ bands listed in Table 1. For each band, the SP/CRDS, Conway/CRDS, HITRAN/CRDS and SP/Conway intensity ratios are plotted *versus* line positions and line intensities. The corresponding average intensity ratios and *rms* deviations are presented in Fig. 8 (note that in the comparison we excluded ratios larger than 2 and smaller than 0.2 and that the average value was calculated as the quadratic mean). SP and Conway intensities show a very good consistency for a number of bands but overall the scattering of the average values is similar to that of the SP/CRDS, Conway/CRDS ratios. The *rms* of the SP/Conway intensity ratios is slightly smaller than that of SP/CRDS. Nevertheless, the intensity ratios of some bands point inaccuracies of both SP and Conway calculated intensities. This is the case of the $4\nu_2$, $5\nu_2$ and $\nu_1+3\nu_2$ bands that we discuss now.

For the $\nu_1+3\nu_2$ transitions, both SP and Conway intensities show a systematic shift. On average, SP intensities are underestimated by 10 % while Conway intensities are overestimated by 15 % (Fig. 7**)** (HITRAN intensities of the $\nu_1+3\nu_2$ transitions were taken from our CRDS study [20]).

The intensity ratios of the $4\nu_2$ band show a larger scattering than those relative to the $\nu_1+3\nu_2$ band, both for SP/CRDS and Conway/CRDS. This is due to the calculated intensity values. Indeed, according to the classification of Refs. [44,56], most of the $4\nu_2$ band transitions are "sensitive" transitions while the $\nu_1+3\nu_2$ band transitions are "stable" transitions. In other words, the intensities of the $4\nu_2$ transitions are very sensitive to small inaccuracies of the PES while it is not the case of the $\nu_1+3\nu_2$ transitions. Overall, SP variational values of the $4\nu_2$ band are closer to experiment than the recent values of Conway et al. We present in Fig. 9 nine examples of comparisons between the various line lists and the CRDS spectra of Refs. [17,18] showing discrepancies of the line intensities. Six of the displayed examples are relative to the $4\nu_2$ band and three concern transitions of the $\nu_1+2\nu_2$ band. Other clear examples were found for transitions of the $5\nu_2$, $\nu_1+\nu_3$ and $6\nu_2$ bands.

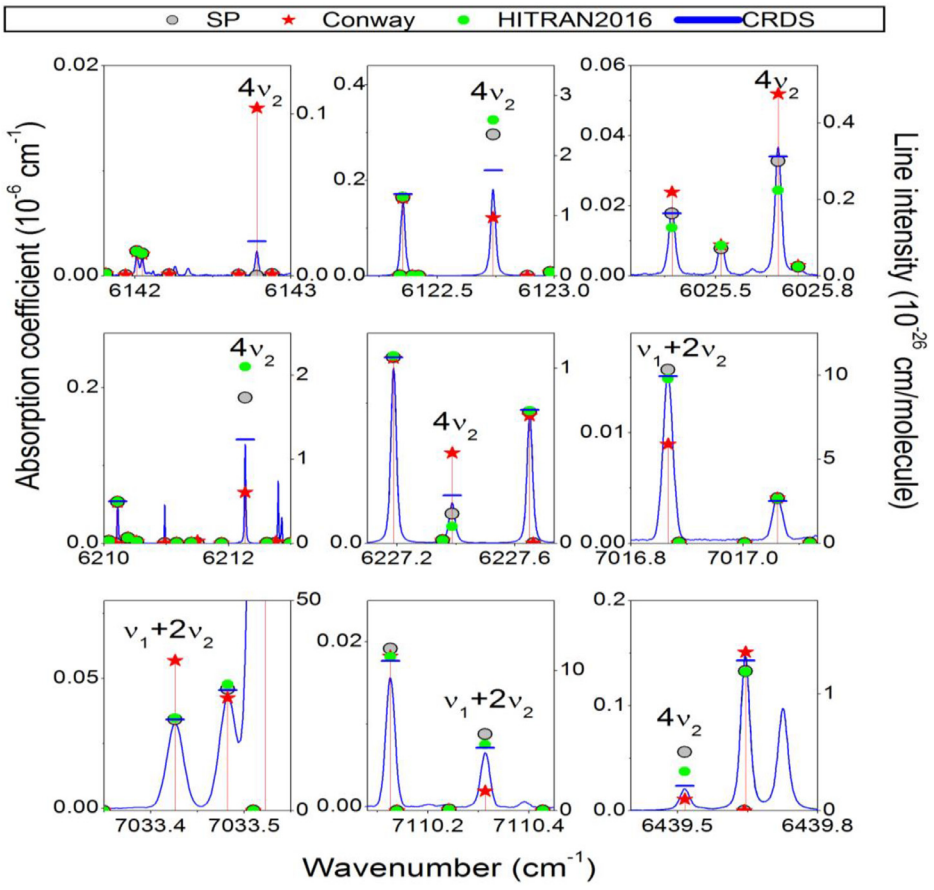

Fig. 9. Examples of disagreement between calculated intensities and the CRDS spectrum of natural water vapor. Line lists of the $H_2{}^{16}O$ main isotopologue as provided by Schwenke and Partridge (full grey circles), by the HITRAN2016 database (full green circles), by Conway et al. [44] (red stars) are compared to CRDS spectra. The blue hyphens correspond to the experimental CRDS intensities as reported in Refs. [17,18]. The problematic lines which belong to the $4\nu_2$ and $\nu_1+2\nu_2$ bands are indicated.

5. Concluding remarks

In recent years, a relatively high number of theoretical line lists have been computed and released for water vapor. Although often called "calculated" line lists, their line positions have an experimental origin and credits should be given to considerable experimental efforts performed over several decades and used to compute their accurate line positions. The direct confrontation of the available line lists produced by different approaches to high quality spectra is a laborious and necessary validation task. Atmospheric validation provides tests in particular for the profile of air-broadened water lines but as concerned line centers, line intensities and completeness, high sensitivity recordings of pure water vapor at low pressure are necessary. In the present work, the CRDS spectra recorded in Grenoble over nearly two decades were used to test the HITRAN2016 list [7] which is the standard list used for atmospheric applications. In the transparency windows, the sensitivity of our CRDS spectrometers allows detecting lines with intensity as small as the 10^{-29} cm/molecule HITRAN intensity cut-off [18]. This is significantly lower than the weakest lines which can be detected in atmospheric spectra. We have also considered in details the lists very recently released by Conway et al. [44] for $H_2{}^{16}O$ and $H_2{}^{18}O$ with intensities calculated from an *ab initio* dipole moment surface. According to the authors, their new dipole moment surface provides excellent calculated intensities and corrects some biases of their preceding POKAZATEL list [55]. Conway et al. indicate that their lists will be used to update many transition intensities and line positions in the HITRAN2016 database [44].

As concerned line positions, the IUPAC-TG approach consisting to collect and evaluate all the position measurements available in the literature in order to derive recommended values of the empirical energy levels by inversion of the transition frequencies using the MARVEL procedure, has proved to be efficient [11–13]. Nevertheless, in absence of direct examination of the spectra, the weighting of frequency values according to their real accuracy is a major issue. As said above the inclusion of a considerable number of transition frequencies reported with multiple assignments from highly congested emission spectra has degraded the quality of part of the IUPAC-TG empirical energy levels.

In the present updated and extended version of the 2016 list of Ref. [38] covering the 5690–8340 cm^{-1} range, the set of empirical energy levels used to compute the line centers has benefited from a large set of new measurements by CRDS referenced to a frequency comb. This CA-CRDS data [25,26] allowed achieving in routine an accuracy of the line center determination at the 10^{-4} cm^{-1} level for well isolated lines. We believe that the line list provided as supplementary material gathers most of the high quality experimental information at disposal for line positions in the considered region. In contrast with the HITRAN2016 and calculated lists, each transition is provided with unique rovibrational labeling (see Fig. 2) and the ambiguities in the vibrational labeling have been resolved using effective Hamiltonian calculations.

The HITRAN database [7] uses six sources for the $H_2{}^{16}O$ line positions in the region (in total, eleven sources for the first six isotopologues). Although, important improvements were incorporated in the 2016 HITRAN list, a number of issues remain to be fixed

concerning erroneous rovibrational assignments (including a number of ortho-para transitions), a small number of missing lines and inaccurate line positions and line intensities. As concerned the recent list of Conway et al. [44], it shows larger deficiencies in terms of line position accuracy. It seems that the set of empirical energy levels used for frequency calculations has to be significantly revised or updated using recent observations. In the considered region, our results clearly indicate that the line positions of the list of Conway et al. should not be used to update the HITRAN list (see Figs. 5 and 6). Other minor issues concerning the list of Conway et al. are that it is limited to J values smaller than 21 and thus some transitions are missing, it includes a high number of duplicate transitions in the $H_2{}^{18}O$ list (263 in our region) and it does not solve the intensity problem of the bending bands (*e.g.* $4\nu_2$, $5\nu_2$, $\nu_1+3\nu_2$) – see Fig. 7.

The laborious evaluation of different theoretical line intensities on the basis of the CRDS recordings of Refs. [14–20] has shown that at present, the line intensities of some bands (in particular the pure bending bands) are predicted satisfactorily by none of the theoretical lists at disposal. For these problematic bands, no important improvements were achieved compared to the twenty-year old results obtained by Schwenke and Partridge [1,2,45] (see Fig. 7).

The best intensity column for water vapor remains thus an open issue for the spectroscopic databases. Compared to measurements, calculations have unique advantages in particular in case of strong line overlapping, very weak lines or for the minor isotopologues. Nevertheless, for some specific bands, all the considered calculated lists show deviations larger than the experimental uncertainty. A possible compromise would be to use calculated intensities as default values and replace them by experimental values when clear deficiencies are evidenced. Taking into account the difficulties to estimate quantitatively the uncertainties on both the calculated and measured intensity values, the criterion of preference between theoretical or experimental intensities remain to be defined.

Declaration of Competing Interest

The authors declare that they have no known competing financial interests or personal relationships that could have appeared to influence the work reported in this paper.

Acknowledgments

E.K. Conway (Center for Astrophysics, Cambridge and University College London) is acknowledged for providing us the submitted version of Ref. [44] together with the corresponding $H_2{}^{16}O$ and $H_2{}^{18}O$ lists, prior publication. The support of the University Grenoble Alpes and CNRS (France) in the frame of International Research Project SAMIA is acknowledged. SNM activity was also partly supported in the frame of the Russian Science Foundation, grant no. 18-11-00024.

Supplementary materials

Supplementary material associated with this article can be found, in the online version, at doi:10.1016/j.jqsrt.2020.106840.

References

[1] Partridge H, Schwenke DW. The determination of an accurate isotope dependent potential energy surface for water from extensive *ab initio* calculations and experimental data. J Chem Phys 1997;106:4618–39.
[2] Schwenke DW, Partridge H. Convergence testing of the analytic representation of an *ab initio* dipole moment function for water: Improved fitting yields improved intensities. J Chem Phys 2000;113:6592–7.
[3] Bubukina II, Polyansky OL, Zobov NF, Yurchenko SN. Optimized semi-empirical potential energy surface for $H_2{}^{16}O$ up to 26000 cm^{-1}. Optics Spectrosc 2011;110:160–6. doi:10.1134/S0030400X11020032.
[4] Conway EK, Kyuberis AA, Polyansky OL, Tennyson J, Zobov N. A highly accurate ab initio dipole moment surface for the ground electronic state of water vapour for spectra extending into the ultraviolet. J Chem Phys 2018;149:084307. doi:10.1063/1.5043545.
[5] Mizus II, Kyuberis AA, Zobov, Makhnev VY, Polyansky OL, Tennyson J. High accuracy water potential energy surface for the calculation of infrared spectra. Phil Trans R Soc Lond A 2018;376:20170149. doi:10.1098/rsta.2017.0149.
[6] Campargue A, Kassi S, Pachucki K, Komasa J. The absorption spectrum of H_2: CRDS measurements of the (2-0) band, review of the literature data and accurate *ab initio* line list up to 35 000 cm^{-1}. Phys Chem Chem Phys 2012;14:802–15. doi:10.1039/C1CP22912E.
[7] Gordon IE, Rothman LS, Hill C, Kochanov RV, Tan Y, Bernath PF, Birk M, Boudon V, Campargue A, Chance KV, Drouin BJ, Flaud J-M, Gamache RR, Hodges JT, Jacquemart D, Perevalov VI, Perrin A, Shine KP, Smith MAH, Tennyson J, Toon GC, Tran H, Tyuterev VlG, Barbe A, Császár AG, Devi VM, Furtenbacher T, Harrison JJ, Hartmann J-M, Jolly A, Johnson TJ, Karman T, Kleiner I, Kyuberis AA, Loos J, Lyulin OM, Massie ST, Mikhailenko SN, Moazzen-Ahmadi N, Müller HSP, Naumenko OV, Nikitin AV, Polyansky OL, Rey M, Rotger M, Sharpe SW, Sung K, Starikova E, Tashkun SA, Vander Auwera J, Wagner G, Wilzewski J, Wcisło P, Yu S, Zak EJ. The HITRAN2016 molecular spectroscopic database. J Quant Spectrosc Radiat Transf 2017;203:3–69.
[8] Jacquinet-Husson N, Armante R, Crépeau N, Chédin A, Scott NA, Boutammine C, Bouhdaoui A, Crevoisier C, Capelle V, Boonne C, Poulet-Crovisier N, Barbe A, Chris Benner D, Boudon V, Brown LR, Buldyreva J, Campargue A, Coudert LH, Devi VM, Down MJ, Drouin BJ, Fayt A, Fittschen C, Flaud J-M, Gamache RR, Harrison JJ, Hill C, Hodnebrong Ø, Hu J-M, Jacquemart D, Jolly A, Jiménez E, Lavrentieva NN, Liu A-W, Lodi L, Lyulin OM, Massie ST, Mikhailenko S, Müller HSP, Naumenko OV, Nikitin A, Nielsen CJ, Orphal J, Perevalov VI, Perrin A, Polovtseva E, Predoi-Cross A, Rotger M, Ruth AA, Yu SS, Sung K, Tashkun SA, Tennyson J, Tyuterev VlG, Vander Auwera J, Voronin BA, Makie A. The 2015 edition of the GEISA spectroscopic database. J Mol Spectrosc 2016;327:31–72.
[9] Furtenbacher T, Császár AG, Tennyson J. MARVEL: measured active rotational-vibrational energy levels. J Mol Spectrosc 2007;245:115–25.
[10] Furtenbacher T, Császár AG. MARVEL: measured active rotational-vibrational energy levels. II. Algorithmic improvements. J Quant Spectrosc Radiat Transf 2012;113:929–35.
[11] Tennyson J, Bernath PF, Brown LR, Campargue A, Carleer MR, Császár AG, et al. IUPAC critical evaluation of the rotational-vibrational spectra of water vapor. Part I. Energy levels and transition wavenumbers for $H_2{}^{17}O$ and $H_2{}^{18}O$. J Quant Spectrosc Radiat Transf 2009;110:573–96.
[12] Tennyson J, Bernath PF, Brown LR, Campargue A, Császár AG, Daumont L, et al. IUPAC critical evaluation of the rotational-vibrational spectra of water vapor. Part II. Energy levels and transition wavenumbers for $HD^{16}O$, $HD^{17}O$, and $HD^{18}O$. J Quant Spectrosc Radiat Transf 2010;111:2160–84.
[13] Tennyson J, Bernath PF, Brown LR, Campargue A, Császár AG, Daumont L, et al. IUPAC critical evaluation of the rotational-vibrational spectra of water vapor. Part III: Energy levels and transition wavenumbers for $H_2{}^{16}O$. J Quant Spectrosc Radiat Transf 2013;117:29–58.
[14] Macko P, Romanini D, Mikhailenko SN, Naumenko OV, Kassi S, Jenouvrier A, et al. High sensitivity CW-cavity ring down spectroscopy of water in the region of the 1.5 μm atmospheric window. J Mol Spectrosc 2004;227:90–108.
[15] Mikhailenko SN, Le Wang, Kassi S, Campargue A. Weak water absorption lines around 1.455 and 1.66 μm by CW-CRDS. J Mol Spectrosc 2007;244:170–8.
[16] Mikhailenko S, Kassi S, Le Wang, Campargue A. The absorption spectrum of water in the 1.25 μm transparency window (7408–7920 cm^{-1}). J Mol Spectrosc 2011;269:92–103.
[17] Leshchishina O, Mikhailenko S, Mondelain D, Kassi S, Campargue A. CRDS of water vapor at 0.1 Torr between 6886 and 7406 cm^{-1}. J Quant Spectrosc Radiat Transfer 2012;113:2155–66.
[18] Leshchishina O, Mikhailenko S, Mondelain D, Kassi S, Campargue A. An improved line list for water vapor in the 1.5 μm transparency window by highly sensitive CRDS between 5852 and 6607 cm^{-1}. J Quant Spectrosc Radiat Transf 2013;130:69–80.
[19] Mikhailenko SN, Karlovets EV, Vasilchenko S, Mondelain D, Kassi S, Campargue A. New transitions and energy levels of water vapor by high sensitivity CRDS near 1.73 and 1.54 μm. J Quant Spectrosc Radiat Transf 2019;236:106574.
[20] Campargue A, Mikhailenko SN, Lohan BG, Karlovets EV, Mondelain D, Kassi S. The absorption spectrum of water vapor in the 1.25 μm atmospheric window (7911 – 8337 cm^{-1}). J Quant Spectrosc Radiat Transf 2015;157:135–52.
[21] Liu A-W, Naumenko OV, Kassi S, Campargue A. CW-Cavity ring down spectroscopy of deuterated water in the 1.58 μm atmospheric transparency window. J Quant Spectrosc Radiat Transf 2014;138:97–106.
[22] Liu A, Naumenko O, Kassi S, Campargue A. High sensitivity CW–CDRS of ^{18}O enriched water near 1.6 μm. J Quant Spectrosc Radiat Transf 2009;110:1781–800.
[23] Mikhailenko SN, Mondelain D, Karlovets EV, Kassi S, Campargue A. Cavity ring down spectroscopy of ^{17}O enriched water vapor near 1.73 μm. J Quant Spectrosc Radiat Transf 2019;222–223:229–35.
[24] Mikhailenko SN, Leshchishina O, Karlovets EV, Mondelain D, Kassi S, Campargue A. CRDS of ^{17}O enriched water between 5850 and 6671 cm^{-1}: more than 1000 energy levels of $H_2{}^{17}O$ and $HD^{17}O$ newly determined. J Quant Spectrosc Radiat Transf 2016;177:108–16.

[25] Mondelain D, Mikhailenko SN, Karlovets EV, Béguier S, Kassi S, Campargue A. Comb-assisted cavity ring down spectroscopy of ^{17}O enriched water between 7443 and 7921 cm^{-1}. J Quant Spectrosc Radiat Transf 2017;203:206–12.
[26] Mikhailenko SN, Mondelain D, Karlovets EV, Kassi S, Campargue A. Comb-assisted cavity ring down spectroscopy of ^{17}O enriched water between 6667 and 7443 cm^{-1}. J Quant Spectrosc Radiat Transf 2018;206:163–71.
[27] Régalia L, Oudot C, Mikhailenko S, Wang L, Thomas X, Jenouvrier A, Von der Heyden P. Water vapor line parameters from 6450 to 9400 cm^{-1}. J Quant Spectrosc Radiat Transf 2014;136:119–36.
[28] Toth RA. Line positions and strengths of HDO between 6000 and 7700 cm^{-1}. J Mol Spectrosc 1997;186:66–89.
[29] Toth RA. Measurements of HDO between 4719 and 5843 cm^{-1}. J Mol Spectrosc 1997;186:276–92.
[30] Naumenko OV, Voronina S, Hu SM. High resolution Fourier transform spectrum of HDO in the 7500-8200 cm^{-1} region: revisited. J Mol Spectrosc 2004;227:151–7.
[31] Tolchenov RN, Tennyson J. Water line parameters for weak lines in the range 7400–9600 cm^{-1}. J Mol Spectrosc 2005;231:23–7.
[32] Jenouvrier A, Daumont L, Régalia-Jarlot L, Tyuterev VlG, Carleer M, Vandaele AC, Mikhailenko S, Fally S. Fourier transform measurements of water vapor line parameters in the 4200–6600 cm^{-1} region. J Quant Spectrosc Radiat Transf 2007;105:326–55.
[33] Mikhailenko SN, Tashkun SA, Putilova TA, Starikova EN, Daumont L, Jenouvrier A, Fally S, Carleer M, Hermans C, Vandaele AC. Critical evaluation of rotation-vibration transitions and an experimental dataset of energy levels of HD^{18}O. J Quant Spectrosc Radiat Transf 2009;110:597–608.
[34] Mikhailenko SN, Tashkun SA, Daumont L, Jenouvrier A, Carleer M, Fally S, Vandaele AC. Line positions and energy levels of the 18-O substitutions from the HDO/D_2O spectra between 5600 and 8800 cm^{-1}. J Quant Spectrosc Radiat Transf 2010;111:2185–96.
[35] Mikhailenko SN, Naumenko OV, Nikitin AV, Vasilenko IA, Liu A-W, Song K-F, et al. Absorption spectrum of deuterated water vapor enriched by ^{18}O between 6000 and 9200 cm^{-1}. J Quant Spectrosc Radiat Transf 2012;113:653–69.
[36] Lisak D, Havey DK, Hodges JT. Spectroscopic line parameters of water vapor for rotation-vibration transitions near 7180 cm^{-1}. Phys Rev A 2009;79:052507.
[37] Sironneau VT, Hodges JT. Line shapes, positions and intensities of water transitions near 1.28 μm. J Quant Spectrosc Radiat Transf 2015;152:1–15.
[38] Mikhailenko SN, Kassi S, Mondelain D, Gamache RR, Campargue A. A spectroscopic database for water vapor between 5850 and 8340 cm^{-1}. J Quant Spectrosc Radiat Transf 2016;179:198–216.
[39] Rothman LS, Gordon IE, Babikov Y, Barbe A, Benner DC, Bernath PF, et al. The HITRAN2012 molecular spectroscopic database. J Quant Spectrosc Radiat Transf 2013;130:4–50.
[40] Kassi S, Stoltmann T, Casado M, Daëron M, Campargue A. Lamb dip CRDS of highly saturated transitions of water near 1.4 μm. J Chem Phys 2018;148:054201.
[41] Régalia L, Thomas X, Rennesson T, Mikhailenko S. Line parameters of water vapour enriched by ^{18}O from 6525 to 8011 cm^{-1}. J Quant Spectrosc Radiat Transf 2019;235:257–71.
[42] Serdyukov VI, Sinitsa LN, Mikhailenko SN. Fourier transform absorption spectrum of ^{17}O enriched water vapour between 7900 and 9500 cm^{-1}. J Quant Spectrosc Radiat Transf 2020 (in preparation).
[43] Tan Y, Mikhailenko SN, Wang J, Liu A-W, Liu G-L, Zhao X-Q, Hu S-M. CRDS absorption spectrum of ^{17}O enriched water vapor in the 12,277–12,894 cm^{-1} range. J Quant Spectrosc Radiat Transf 2018;221:233–42.
[44] Conway EK, Gordon IE, Kyuberis AA, Polyansky OL, Tennyson J, Zobov NF. Calculated line lists for $H_2{}^{16}O$ and $H_2{}^{18}O$ with extensive comparisons to theoretical and experimental sources including the HITRAN2016 database. J Quant Spectrosc Radiat Transf 2020;241:106711. doi:10.1016/j.jqsrt.2019.106711.
[45] Tashkun SA. Institute of Atmospheric Optics SB RAS. 2007. http://spectra.iao.ru/molecules/simlaunch?mol=1.
[46] Naumenko O, Leshchishina O, Campargue A. High sensitivity absorption spectroscopy of HDO by ICLAS-VeCSEL between 9100 and 9640 cm^{-1}. J Mol Spectrosc 2006;236:58–69.
[47] Mellau GCh, Mikhailenko SN. Rotational levels of five lowest states of $H_2{}^{18}O$ and $H_2{}^{17}O$ from hot emission spectra between 320 and 2500 cm^{-1}, in preparation.
[48] Liu A-W, Song K-F, Ni H-Y, Hu S-M, Naumenko OV, Vasilenko IA, Mikhailenko SN. (000) and (010) energy levels of the HD^{18}O and $D_2{}^{18}O$ molecules from analysis of their ν_2 bands. J Mol Spectrosc 2011;265:26–38.
[49] Mellau GCh, Mikhailenko SN, Tyuterev VlG. Hot water emission spectra: rotational energy levels of the (000) and (010) states of HD^{17}O. J Mol Spectrosc 2015;308–309:6–19.
[50] Tyuterev VlG, Starikov VI, Tashkun SA, Mikhailenko SN. Calculation of high rotation energies of the water molecule using the generating function model. J Mol Spectrosc 1995;170:38–58.
[51] Vasilchenko S, Tran H, Mondelain D, Kassi S, Campargue A. Accurate absorption spectroscopy of water vapor near 1.64 mm in support of the MEthane Remote LIdar missioN (MERLIN). J Quant Spectrosc Radiat Transf 2019;235:332–42.
[52] Barber RJ, Tennyson J, Harris GJ, Tolchenov RN. A high-accuracy computed line list. Mon Not R Astron Soc 2006;368:1087–94.
[53] Lodi L, Tennyson J, Polyansky OL. A global, high accuracy *ab initio* dipole moment surface for the electronic ground state of the water molecule. J Chem Phys 2011;135:034113.
[54] Toth RA. Line list of water vapor parameters from 500 to 8000 cm−1, http://mark4sun.jpl.nasa.gov/h2o.html.
[55] Polyansky OL, Kyuberis AA, Zobov NF, Tennyson J, Yurchenko SN, Lodi L. ExoMol molecular line lists XXX: a complete high-accuracy line list for water. Mon Not Roy Astron Soc 2018;480:2597–608. doi:10.1093/mnras/sty1877.
[56] Lodi L, Tennyson J. Line lists for $H_2{}^{18}O$ and $H_2{}^{17}O$ based on empirical line positions and ab initio intensities. J Quant Spectrosc Radiat Transf 2012;113:850–858.